Supporting Information

Robust large-area molecular junctions based on transparent and flexible electrodes

Aitor García-Serrano,[a,b] Pilar Cea,[a,b,c*] Henrry M. Osorio,[d] Francesc Pérez-Murano,[e] Gemma Rius,[e] Paul J. Low,[f] Santiago Martin,[a,b,c*]

[a] *Instituto de Nanociencia y Materiales de Aragón (INMA), Universidad de Zaragoza-CSIC, 50009 Zaragoza, Spain.*

[b] *Departamento de Química Física, Facultad de Ciencias, Universidad de Zaragoza, 50009, Zaragoza, Spain.*

[c] *Laboratorio de Microscopias Avanzadas (LMA) Campus Río Ebro, Universidad de Zaragoza, C/ Mariano Esquilor, s/n, 50018 Zaragoza, Spain.*

[d] *Departamento de Física, Escuela Politécnica Nacional, Av. Ladrón de Guevara, E11-253, 170525 Quito, Ecuador*

[e] *Instituto de Microelectrónica de Barcelona (IMB-CNM, CSIC), Campus UAB, 08193 Bellaterra, Spain.*

[f] *School of Molecular Sciences, University of Western Australia, 35 Stirling Highway, Crawley, Perth, 6009, Australia.*

S1. Optimization of the PEDOT:PSS deposition on Mylar®

To achieve the optimum conditions for the deposition of a PEDOT:PSS solution on Mylar®, both the spin-coating parameters (steps, time, and speed) and the addition of additives (to improve the conductivity, reduce the roughness and increase the chemical and physical resistance) were evaluated; the obtained data are summarized below (Table S1 and S2).

Table S1. Root mean square, RMS, roughness values obtained by AFM for several Mylar-PEDOT:PSS substrates depending on the spin coating parameters.

Mylar-PEDOT:PSS	r.p.m. (s)	RMS roughness /nm
1	500 (5) / 2000 (60)	1.65 ± 0.08
2	500 (5) / 3000 (60)	1.59 ± 0.06
3	500 (5) / 4000 (60)	1.48 ± 0.05
4	500 (5) / 5000 (60)	1.50 ± 0.06

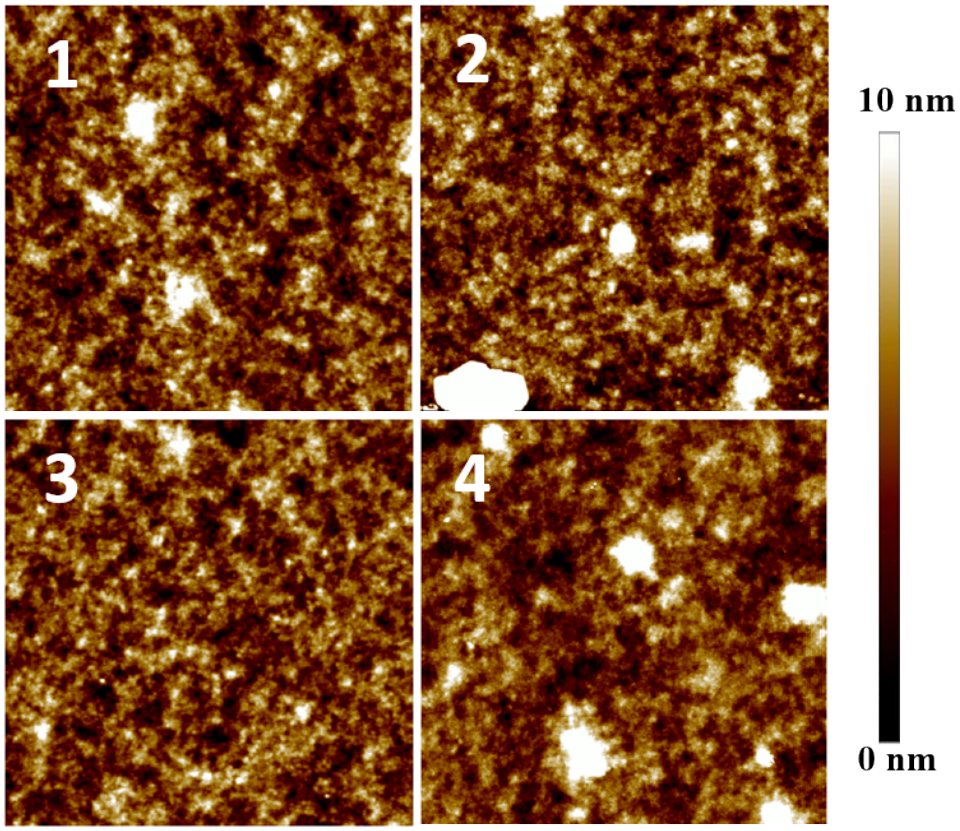

Figure S1. 5x5 μm^2 AFM images for Mylar-PEDOT:PSS substrates under the deposition conditions shown in Table S1.

Table S2. Root mean square, RMS, roughness values obtained by AFM for several Mylar-PEDOT:PSS substrates depending on the added additives. PEDOT:PSS was deposited by spin-coating in two subsequent steps at 500 (5 s) and 4000 (60 s) rpm.

Mylar-PEDOT:PSS	GOPS (%)	DMSO (%)	EG (%)	RMS roughness/nm
1	5	2.5	-	1.60 ± 0.11
2	0.1	2.5	-	1.50 ± 0.10
3	5	-	2.5	1,55 ± 0.08
4	0.1	-	2.5	1.30 ± 0.06

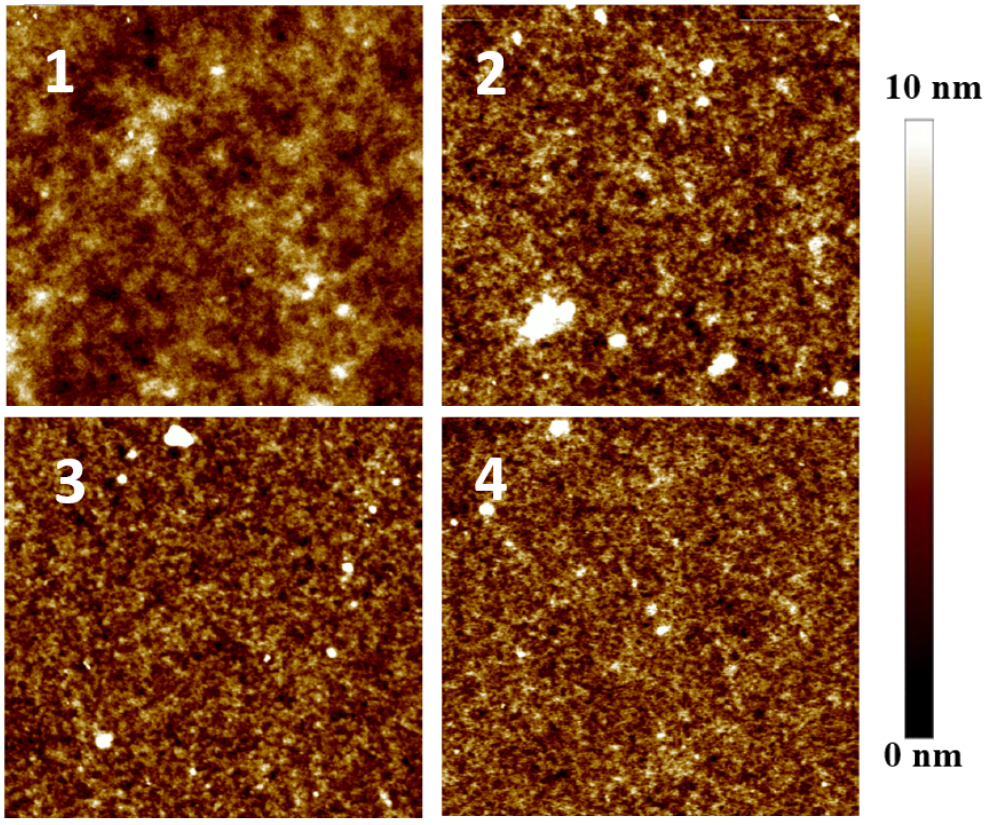

Figure S2. 5x5 μm^2 AFM images for Mylar-PEDOT:PSS substrates under the conditions shown in Table S2.

S2. Elimination of the TMS group after the electrografting process

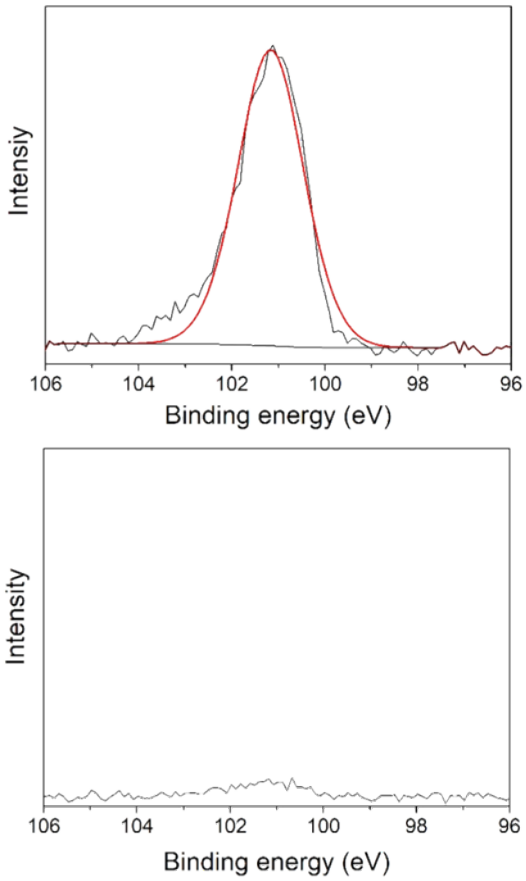

Figure S3. XPS of the Si2p region for a electrografted monolayer of compound **1** on Mylar-PEDOT:PSS before (top) and after (bottom) removing the TMS group.

S3. Determination of the electrografted film thickness

The thickness of the electrografted layer was estimated by scratching the surface with the AFM tip to reveal the underlying bare HOPG surface followed by measurement of the cross section and depth profiles across the scratched area (Figure S4). A film thickness of 2.1 ± 0.2 nm was obtained.

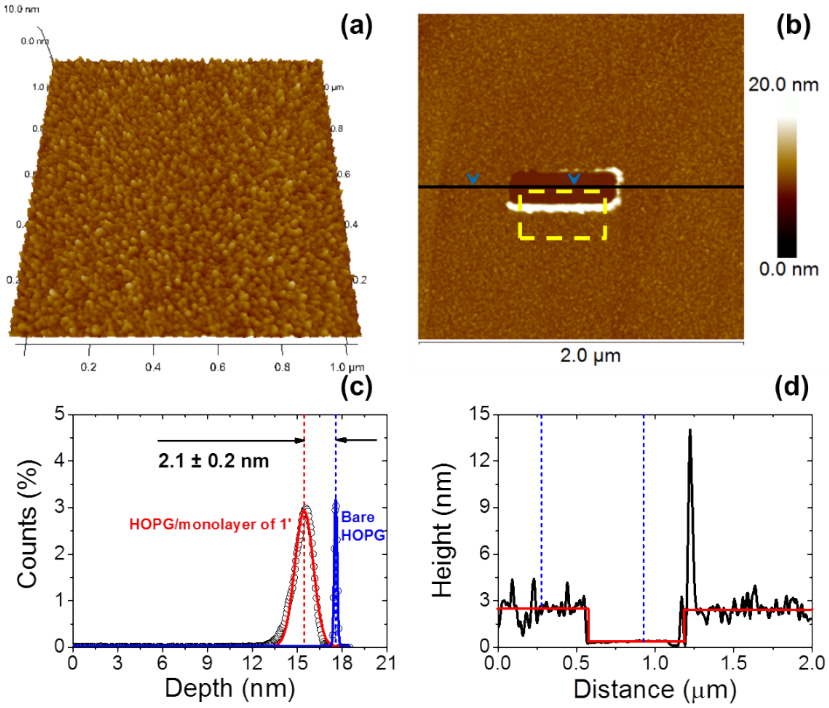

Figure S4. (a) AFM image showing the topography of a HOPG/grafted monolayer. (b). AFM image of a 500 x 125 nm^2 scratch made in the organic film. (c) Depth profile histogram corresponding to the dashed yellow-boxed 400 x 100 nm^2 area, exhibiting the depth value distributions related to HOPG bare surface, blue line, and the organic monolayer, red line. (d) Representative cross-section profile across the scratched area.

S4. Raman Spectroscopy

Raman spectroscopy was used to determine whether the electrografting process could affect the properties of the underlying PEDOT:PSS layer. The bands observed in the Raman spectra (Figure S5) arise from the PEDOT and PSS components of the conducting layer.[1-4] The similarity observed in the Raman spectra before and after the electrografting process (once the TMS group was removed) confirms that this process does not alter the PEDOT:PSS characteristics.

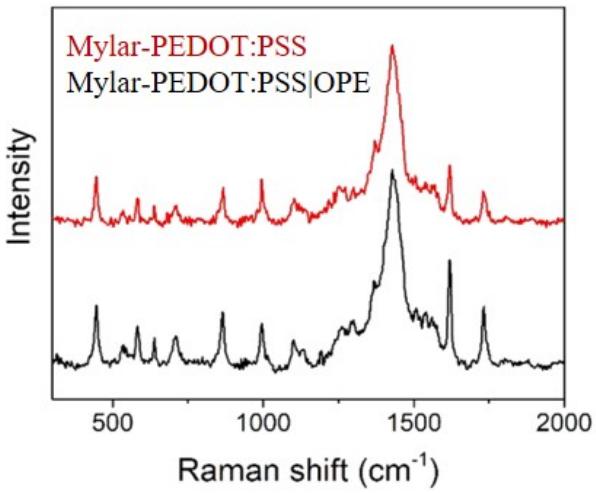

Figure S5. Raman spectrum for the Mylar-PEDOT:PSS (red) and Mylar-PEDOT:PSS|OPEH structure (black).

S5. Electrochemical Characterization

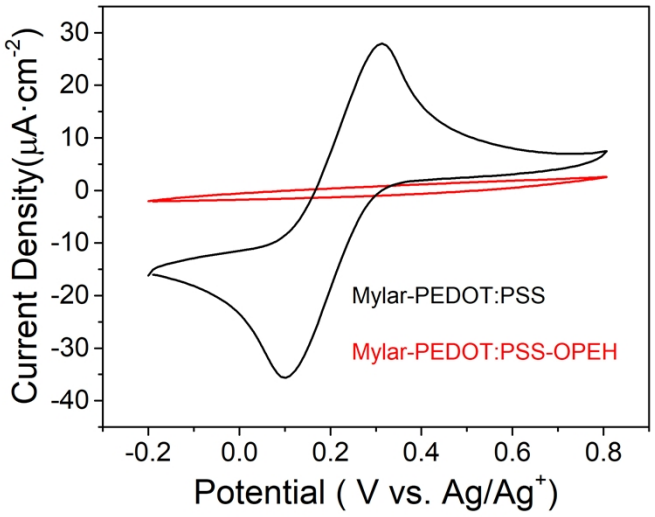

Figure S6. Cyclic voltammograms recorded at 0.05 $V \cdot s^{-1}$ for a Mylar-PEDOT:PSS and Mylar-PEDOT:PSS|OPEH substrate in a 1 mM ferrocyanide + 0.1 M KCl solution.

S6. Graphene as a large top contact electrode

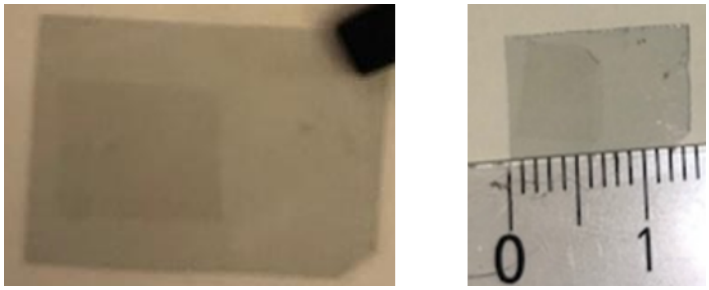

Figure S7. Photograph images showing the large graphene layer, ca. 0.7 x 0.6 cm (top-contact electrode) onto a Mylar-PEDOT:PSS|OPEH substrate.

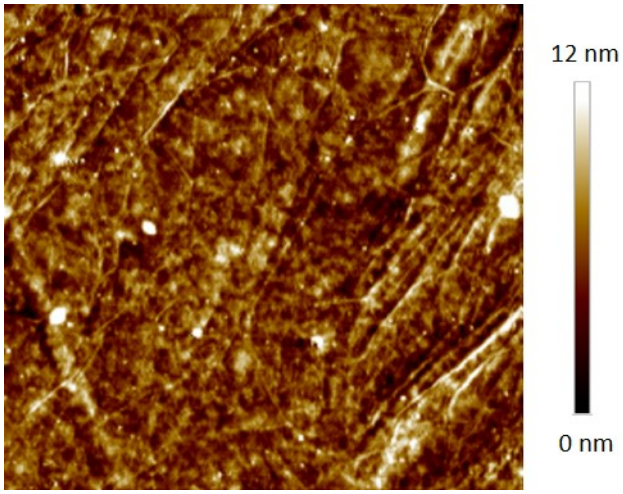

Figure S8. 5x5 μm^2 topography AFM image for a Mylar-PEDOT:PSS|Graphene substrate; the observed bright spots are traces of residual PMMA.

S7. I-V curves for a Mylar-PEDOT:PSS|Graphene substrate

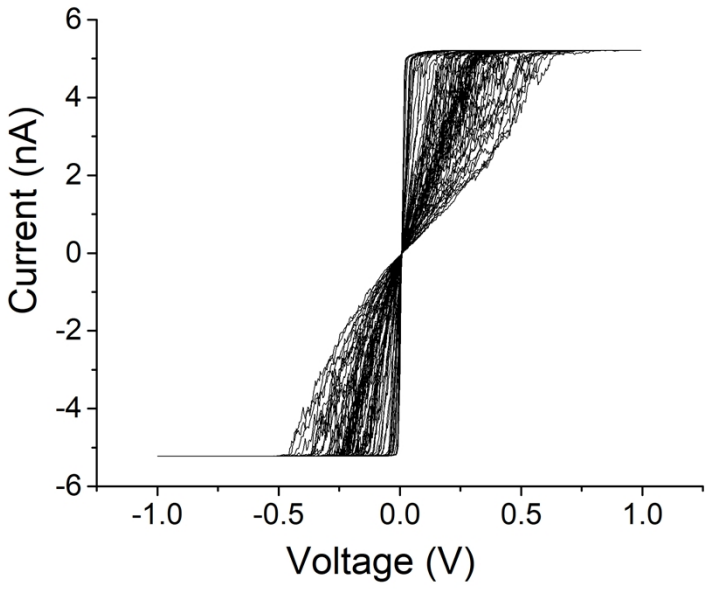

Figure S9. *I-V* curves (ca. 80) recorded at 10 nN from several different areas of the Mylar-PEDOT:PSS|Graphene substrate.

S8. I-V curves after folding and stretching the Mylar-PEDOT:PSS|OPEH|Graphene substrate

Figure S10 shows 60 *I-V* curves recorded at 11 and 15 nN set points from several different areas of the device (with the average of these curves in red) recorded after the Mylar-PEDOT:PSS|OPEH|Graphene substrate was folded and stretched.

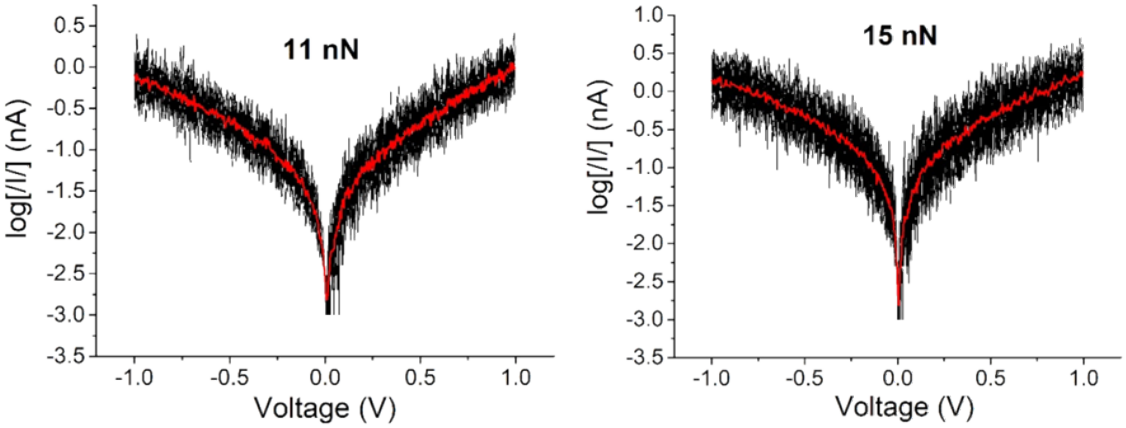

Figure S10. Log[|*I*|] versus voltage for 60 *I–V* curves measured at a set point force of 11 nN (left) and 15 nN (right) recorded after the substrates were folded and stretched. The red line shows the average curve in each case.

S9. References

1. S. Garreau, J. L. Duvail and G. Louarn, *Synth. Met.*, 2001, **125**, 325-329.
2. M. Stavytska-Barba and A. M. Kelley, *J. Phys. Chem. C*, 2010, **114**, 6822-6830.
3. Y. K. Han, M. Y. Chang, W. Y. Huang, H. Y. Pan, K. S. Ho, T. H. Hsieh and S. Y. Pan, *J. Electrochem. Soc.*, 2011, **158**, K88-K93.
4. A. A. Farah, S. A. Rutledge, A. Schaarschmidt, R. Lai, J. P. Freedman and A. S. Helmy, *J. Appl. Phys.*, 2012, **112**, 113709.